ChemInform Abstract: Synthesis and Characterization of the Electronic and Electrochemical Properties of Thienylenevinylene Oligomers with Multinanometer Dimensions.

ARTICLE *in* CHEMINFORM · AUGUST 1998

Impact Factor: 0.74 · DOI: 10.1021/ja980603z

6 AUTHORS, INCLUDING:

Pierre Frère
University of Angers
129 PUBLICATIONS **3,294** CITATIONS
SEE PROFILE

Jean Roncali
French National Centre for Scientific Research
347 PUBLICATIONS **14,332** CITATIONS
SEE PROFILE

Synthesis and Characterization of the Electronic and Electrochemical Properties of Thienylenevinylene Oligomers with Multinanometer Dimensions

Isabelle Jestin,[†] Pierre Frère,[†] Nicolas Mercier,[†] Eric Levillain,[†] Didier Stievenard,[‡] and Jean Roncali*,[†]

Contribution from the Ingénierie Moléculaire et Matériaux Organiques, CNRS UMR 6501, Université d'Angers, 2 Boulevard Lavoisier, F-49045 Angers, France, and Institut d'Electronique et de Microélectronique du Nord, Avenue Poincaré BP 69, F-59652 Villeneuve d'Ascq, France

Received February 23, 1998

Abstract: Soluble thienylenevinylene oligomers based on 3,4-dihexylthiophene with chain length approaching 100 Å (16-mer) have been synthesized. Optical data obtained in solution and on solution-processed thin films show that chain extension produces a narrowing of the HOMO−LUMO gap (ΔE) and band gap (E_g) which reach values significantly smaller than that of the parent polymer. Plots of ΔE and E_g vs the reciprocal number of carbons in the chain (1/Cn) reveal a deviation from linearity beyond the 10−12-mer suggesting a limit of convergence around the 20−22-mer. Cyclic voltammetry shows that chain lengthening induces a negative shift of the first redox potential, an increase of the number of accessible redox states, and a decrease of the Coulombic repulsion in multicationic species. Thus, the 16-mer can be charged up to the hexacationic state within a 0.60-V potential window. A plot of the potential of the various redox steps vs 1/Cn suggests full coalescence into a single-step process for the 20−22-mer. A single process is indeed observed for solution cast films of 16-mer, and the respective contributions of the intra- and intermolecular mechanisms in the recombination process are discussed.

Introduction

The control of the structure and electronic properties of linear π-conjugated systems with multinanometer dimensions and well-defined chemical structure is the focus of considerable current interest.[1] In addition to their use as advanced materials for electronic or photonic applications,[2,3] these compounds have been intensively investigated to model the electronic and electrochemical properties of the parent polydisperse polymer.[4] While these research areas remain very active, the past few years have witnessed the rapid emergence of a widespread interest related to the use of π-conjugated oligomers as molecular wires in molecular electronic devices.[5] Such a purpose requires stable linear π-conjugated systems combining optimal π-electron delocalization with dimensions approaching the present limit of nanolithographic techniques i.e., the 100-Å regime. Although simple polyenic structures should in principle exhibit optimal π-electron delocalization, their lack of chemical and photothermal stability represents a major drawback. Recently, more stable π-conjugated oligomers based on thiophene,[4f] triacetylene,[4g] phenylenevinylene,[4h] phenyleneethynylene,[1c] and thiophene-ethynylene[5g] have been synthesized, and chain lengths reaching the hexadecamer stage and dimensions sometimes exceeding 100 Å have been reported.[1c,5g,h] However, all these structures exhibit a more or less rapid saturation of the effective conjugation length (ECL). Consequently, the width of the HOMO−LUMO and band gaps converge toward a constant limit for chain lengths significantly shorter than the maximum chain dimension. Since this saturation effect originates from π-electron confinement related to structural factors such as rotational disorder or resonance stabilization energy,[1b,6] more planar and less aromatic oligomeric structures may exhibit improved π-electron delocalization.

Although the excellent charge-transmission properties of thienylenevinylene oligomers (nTVs) have been demonstrated in NLO chromophores[7] or extended tetrathiafulvalene ana-

[†] Université d'Angers.

[‡] Institut d'Electronique et de Microélectronique du Nord.

(1) (a) *Handbook of Conducting Polymers*; Elsenbaumer R. L., Skotheim, T., Reynolds, J. R., Eds.; Dekker: New York, 1998. (b) Roncali, J. *Chem. Rev.* **1997**, *97*, 173. (c) Tour, J. M. *Chem. Rev.* **1996**, *96*, 537.

(2) (a) Tasaka, S.; Katz, H. E.; Hutton, R. S.; Orenstein, J.; Frederickson, G. H.; Wang, T. T. *Synth. Met.* **1986**, *16*, 17. (b) Garnier, F.; Hajlaoui, R.; Yassar, A.; Srivastava, P. *Science* **1994**, *265*, 1684. (c) Dodabalapur, A.; L. Torsi, L.; Katz, H. E. *Science* **1995**, *268*, 270. (d) Katz, H. E. *J. Mater. Chem.* **1997**, *7*, 369.

(3) Geiger, F.; Stoldt, M.; Schweizer, R.; Bäuerle, P.; Umbach, E. *Adv. Mater.* **1993**, *5*, 922.

(4) (a) Jones, D.; Guerra, M.; Favaretto, L.; Modelli, A.; Fabrizio, M.; Distefano, G. *J. Phys. Chem.* **1990**, *94*, 5761. (b) Caspar, J. V.; Ramamurthy, V.; Corbin, D. R. *J. Am. Chem. Soc.* **1991**, *113*, 600. (c) Havinga, E. E.; Rotte, I.; Meijer, E. W.; ten Hoeve, W.; Wynberg, H. *Synth. Met.* **1991**, *41*, 473. (d) Bäuerle, P. *Adv. Mater.* **1992**, *4*, 102. (e) Guay, J.; Kasai, P.; Diaz, A.; Wu, R.; Tour, J. M.; Dao, L. H. *Chem. Mater.* **1992**, *4*, 1097. (f) Bäuerle, P.; Fisher, T.; Bidlingmeier, B.; Stabel, A.; Rabe, J. P. *Angew. Chem., Int. Ed. Engl.* **1995**, *34*, 303. (g) Martin, R. E.; Gubler, U.; Boudon, C.; Gramlich, V.; Bosshard, C.; Gisselbrecht, J.-P.; Günter, P.; Gross, M.; Diederich, F. *Chem. Eur. J.* **1997**, *3*, 1505. (h) Stalmach, U.; Kolshorn, H.; Brehm, I.; Meier, H. *Liebigs Ann. Chem.* **1996**, 1449.

(5) a) Lehn, J. M. *Angew. Chem., Int. Ed. Engl.* **1988**, *27*, 90. (b) Aviram, A. *J. Am. Chem. Soc.* **1988**, *110*, 5687. (c) Effenberger, F.; Schlosser, H.; Bäuerle, P.; Maier, S.; Port, H.; Wolf, H. C. *Angew. Chem., Int. Ed. Engl.* **1988**, *27*, 281. (d) Guay, J.; Diaz, A.; Wu, R.; Tour, J. M. *J. Am. Chem. Soc.* **1993**, *115*, 1869. (e) Beley, M.; Chodorowski-Kimmes, Collin, J. P.; Lainé, P.; Launay, J. P.; Sauvage, J. P. *Angew. Chem., Int. Ed. Engl.* **1994**, *33*, 1775. (f) Grosshenny, V.; Harriman, A.; Ziessel, R. *Angew. Chem., Int. Ed. Engl.* **1995**, *34*, 1100. (g) Pearson, D. L.; Schumm, J. S.; Tour, J. M. *Macromolecules* **1994**, *27*, 2348. (h) Wu, R.; Schumm, J. S.; Pearson, D. L.; Tour, J. M. *J. Org. Chem.* **1996**, *61*, 6906.

S0002-7863(98)00603-9 CCC: $15.00
Published on Web 07/31/1998

Chart 1

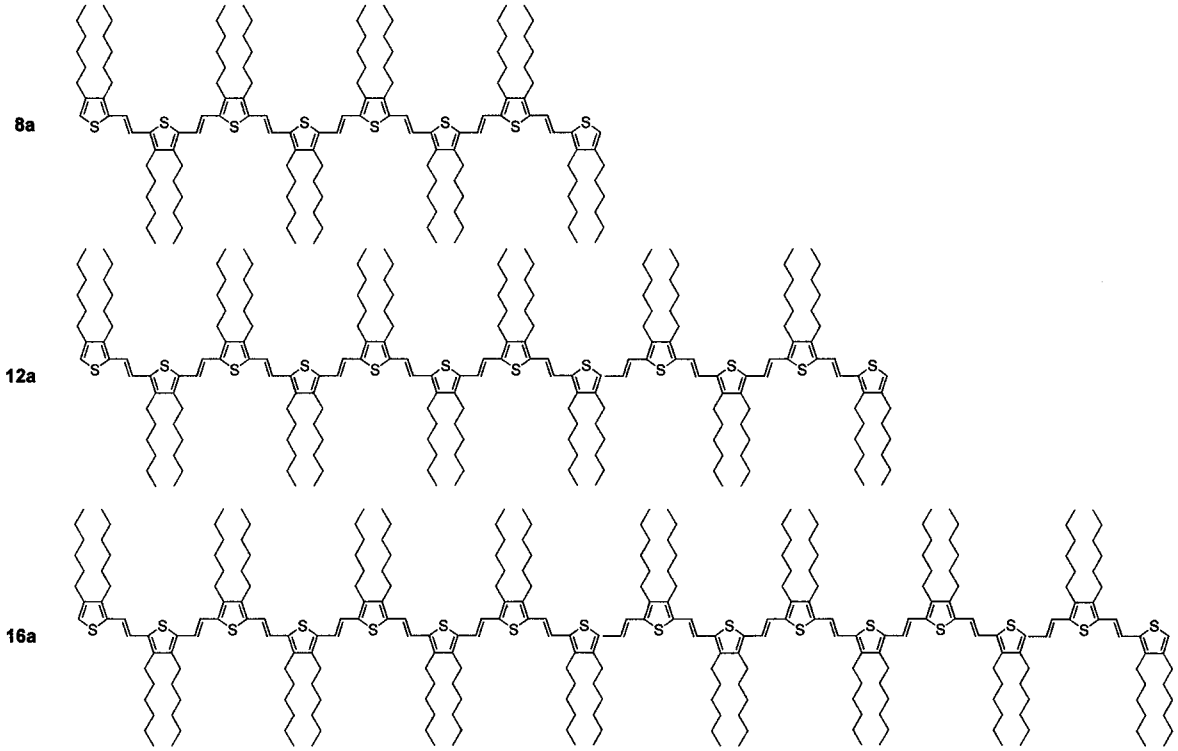

logues,[8] this class of π-conjugated oligomers has attracted only limited attention so far. Unsubstituted nTVs up to $n = 7$ were first prepared by Kossmehl et al. in the late 1970s.[9] More recently these compounds have been synthesized by other groups,[10] while some cyclic versions of nTVs have been developed by Cava et al.[11] As shown by these various works, the rapid decrease of solubility with chain length has so far hindered the synthesis of longer nTVs and the detailed analysis of their electronic and electrochemical properties.

Recently, we reported the synthesis of soluble nTVs based on 3-octylthiophene and 3,4-dibutylthiophene, and we analyzed the chain length dependence of their electrochemical and electronic properties.[12] Although no saturation of ECL was observed up to the decamer stage, further chain extension was again hampered by solubility problems.[12b] Consequently, the ultimate values of quantities such as ECL, oxidation potential, HOMO−LUMO gap, and band gap are still to be determined.

In an attempt to solve these problems, we report here the synthesis and characterization of nTVs based on 3,4-dihexylthiophene.[13] The enhanced solubility of these oligomers allows chain extension up to the hexadecamer stage and to dimensions approaching 100 Å (Chart 1). The chain length dependence of the electrochemical and optical properties has been analyzed in solution and in the solid state, and the relevance of these novel nTVs as models for the corresponding polymer or as molecular wires is discussed.

Results and Discussion

The synthesis of the target oligomers is depicted in Scheme 1. We have previously reported the synthesis of nTVs from the dimer to the decamer[12] by means of a combination of formylation reaction and McMurry dimerization.[14] However, as chain length increases, selective monoformylation becomes increasingly difficult and, for instance, formylation of the tetramer invariably produced a mixture of mono- and dialdehydes difficult to separate. To circumvent this problem we adopted here a different strategy based on double formylation followed by 2-fold Wittig−Horner olefination of the resulting dialdehyde. Thus, except for the dimer and tetramer **2a** and **4a**, prepared by McMurry coupling, all longers nTVs have been synthesized by double Wittig−Horner olefination with phosphonate **2e**. This leads to an increase of chain length by four units at each iterative step. 3,4-Dihexylthiophene (**1a**) was synthesized from 3,4-dibromothiophene by nickel-catalyzed cross-coupling with bromohexylmagnesium reagent.[15] Vilsmeier formylation of **1a** gave aldehyde **1b** in 88% yield. McMurry coupling of aldehyde **1b** afforded dithienylethylene **2a** in 74% yield. Monoaldehyde **2b** was prepared in 86% yield by Vilsmeier formylation of **2a**. The use of a large excess of DMF afforded the dicarbaldehyde **2c** in 88% yield. Reduction

(6) (a) Alberti, A.; Favaretto, L.; Seconi, G. *J. Chem. Soc., Perkin Trans. 2* **1990**, 931. (b) Chadwick, J. E. Kohler, B. E. *J. Phys. Chem.* **1994**, *98*, 3631. (c) Distefano, G.; Da Colle, M.; Jones, D.; Zambianchi, M.; Favaretto, L.; Modelli, A. *J. Phys. Chem*. **1993**, *97*, 3504. (d) Orti, E.; Viruela, P. M.; Sanchez-Marin, J.; Tomas, F. *J. Phys. Chem.* **1995**, *99*, 4955. (e) Horne, J. C.; Blanchard, G. J.; LeGoff, E. *J. Am. Chem. Soc.* **1995**, *117*, 955.

(7) (a) Rao, V. P.; Jen, A. K.-Y.; Wong, K. Y.; Drost, K. J. *Tetrahedron Lett.* **1993,** *34*, 1747. (b) Rao, V. P.; Cai, Y. M.; Jen, A. K.-Y. *J. Chem. Soc., Chem. Commun.* **1994**, 1689.

(8) (a) Roncali, J. *J. Mater. Chem*. **1997**, *12*, 2037. (b) Elandaloussi, E.; Frère, P.; Roncali, J.; Richomme, P.; Jubault, M.; Gorgues, A. *Adv. Mater.* **1995**, *7*, 390. (c) Elandaloussi, E.; Frère, P.; Roncali, J. *Tetrahedron Lett.* **1996**, *37*, 6121.

(9) (a) Kossmehl, G. *Ber. Bunsen-Ges. Phys. Chem*. **1979**, *83*, 417. (b) Kossmehl, G.; Härtel, M.; Manecke, G. *Makromol. Chem.* **1970**, *131*, 15.

(10) (a) Nakayama J.; Fujimori, T. *Heterocycles* **1991**, *32*, 991. (b) Spangler, C. W.; Liu, P.-K. *Synth. Met.* **1991**, *44*, 259. (c) Spangler, C. W.; Bryson, P.; Liu, P.-K.; Dalton, L. R. *J. Chem. Soc., Chem. Commun.* **1992**, 253.

(11) Hu, Z.; Atwood, J. L.; Cava, M. P. *J. Org. Chem.* **1994**, *59*, 8071.

(12) (a) Elandaloussi, E.; Frère, P.; Roncali, J. *Chem. Commun*. **1997**, 301. (b) Elandaloussi, E.; Frère, P.; Richommme, P.; Orduna, J.; Garin, J.; Roncali, J. *J. Am. Chem. Soc*. **1997**, *119*, 10774.

(13) Preliminary communication: Jestin, I.; Frère, P.; Blanchard, P.; Roncali, J. *Angew. Chem., Int. Ed.* **1998**, *37*, 942.

(14) McMurry, J. E. *Chem. Rev.* **1989**, *89*, 1513. Fürstner, A.; Bogdanovic, B. *Angew. Chem., Int. Ed. Engl*. **1996**, *35*, 2443.

(15) Tamao, K.; Odama, S.; Nakasima, I.; Kumada, M.; Minato, A.; Suzuki, K. *Tetrahedron* **1982**, *8*, 3347.

Scheme 1[a]

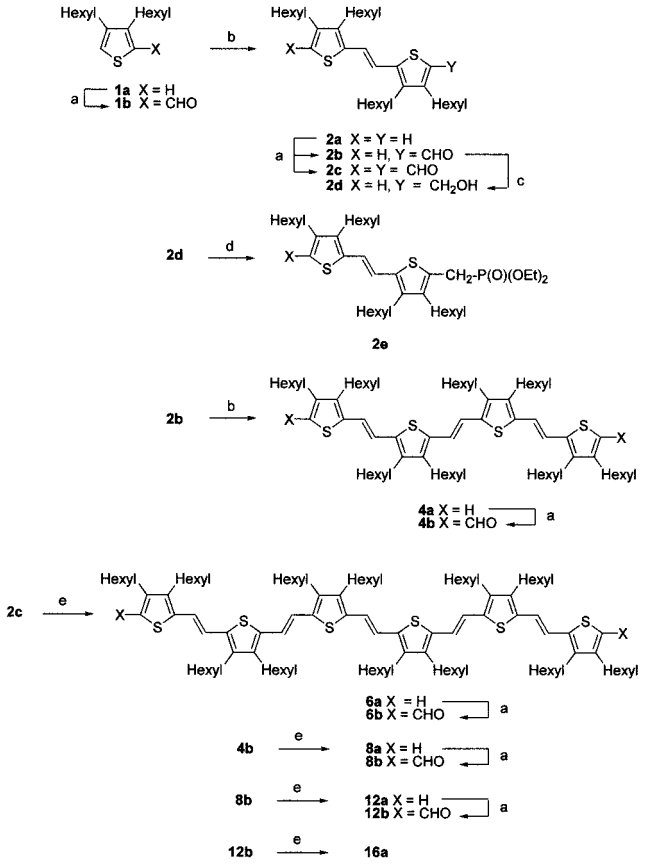

[a] Reagents and conditions: (a) $POCl_3$, DMF/DCE, reflux; (b) $TiCl_4$, Zn/THF, reflux; (c) $NaBH_4/CH_2Cl_2$−methanol, room temperature; (d) PBr_3/toluene−benzene −5 °C, then NaH and $HP(OEt)_2$/THF −20 °C, then reflux; (e) *t*-BuOK/THF room temperature.

of **2c** with $NaBH_4$ gave the alcohol **2d** in 91% yield. Phosphonate **2e** was then prepared by reaction of **2d** with PBr_3 to produce the corresponding bromo derivative, which was immediately reacted with the anion of diethyl phosphite to give the target Wittig−Horner reagent in 73% yield. McMurry coupling of the carbaldehyde **2b** afforded the tetramer **4a** in 86% yield. This compound was converted into the corresponding dicarbaldehyde **4b** by Vilsmeier formylation. The hexamer **6a** was prepared in 84% yield by Wittig−Horner olefination of the dialdehyde **2c** with **2e**. Conversion of **6a** into the dialdehyde **6b** (yield 70%) and repetition of the whole procedure led successively to the octamer **8a**, dodecamer **12a**, and hexadecamer **16a** in 64, 55, and 30% yield, respectively.

All nTVs were satisfactorily characterized by NMR, mass, and UV−visible spectroscopies. In particular the all-trans configuration of all double bonds was confirmed by comparison of the UV−visible spectra (steady red shift of λ_{max}, absence of cis band, well-resolved vibronic fine structure) with those of partially substituted nTVs for which the all-trans structure was previously established by ^{1}H NMR.[12b] Due to the sensitivity of long nTVs toward light and oxygen, correct combustion analyses were extremely difficult to obtain in some cases and required that the samples be kept under argon and analyzed shortly after synthesis. Consequently, electrochemical and spectroscopic experiments were performed on freshly purified samples.

To gain more detailed information about the structure, the growth of single crystals of nTVs was attempted. However, crystals of quality sufficient for X-ray determination could be obtained only in the case of the tetrameric dialdehyde **4b**. Figure 1 shows the ORTEP view of **4b**. The side view confirms the perfect planarity of the π-conjugated system although every second hexyl chain lies outside the plane of the π-conjugated system while the corresponding carbons present large thermal ellipsoids. Extrapolation of the chain length of **4b** leads to an estimated length of 96 Å for **16a**, in excellent agreement with the 95 Å obtained by optimization of the geometry by the MM$^+$ method.[16]

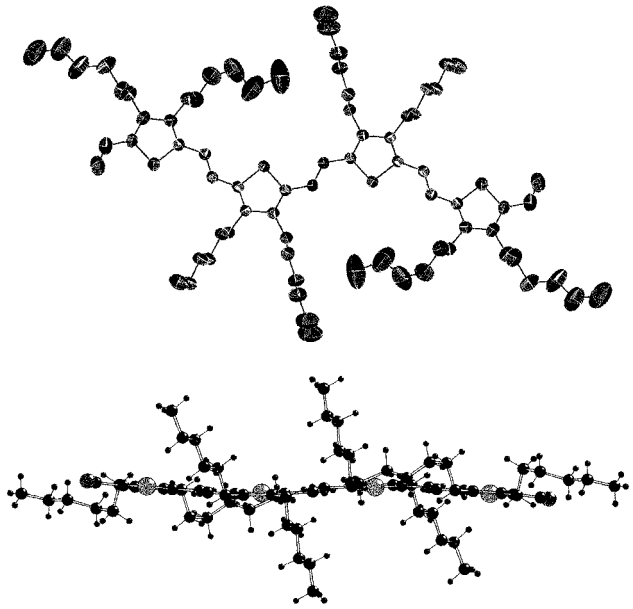

Figure 1. ORTEP view of the dialdehyde **4b**.

Table 1. UV−Visible Spectroscopic Data for nTVs in CH_2Cl_2

compd	λ_{max} (nm)	ϵ	ΔE^a (eV)[a]	$\lambda_{0-0}{}^b$ (nm)	$E_g{}^b$ (eV)	Cn
2	360	18 000	3.30	383	3.01	10
4a	489	69 500	2.39	542	2.05	22
6a	548	109 000	2.12	621	1.80	34
8a	574	156 000	2.00	651	1.68	46
12a	595	206 000	1.95	676	1.60	70
16a	601	319 000	1.93	682	1.56	94

[a] From the maximum of the 0-0 transition. [b] On films.

Electronic Absorption Spectroscopy. Table 1 lists the main electronic absorption data for the various nTVs in solution and in the solid state. Chain extension leads to the expected bathochromic shift of the absorption maximum (λ_{max}), to a narrowing of the HOMO−LUMO gap (ΔE)[17] and to an increase of the molecular extinction coefficient (ϵ). Thus, for **16a**, λ_{max} and ϵ reach values of 601 nm and 319 000 mol L^{-1} cm^{-1}, respectively, which are by far the largest ever reported for a π-conjugated oligomer of homogeneous chemical structure.

The UV−visible spectra of **4a**, **8a**, and **16a** are shown in Figure 2. In each case the spectrum retains a well-resolved vibronic fine structure indicative of the persistence of a relatively planar and rigid geometry even for the longest chains. The equally spaced maximums (0.15−0.17 eV) are consistent with a C=C stretching mode strongly coupled to the electronic

(16) Hyperchem 5.0, Hypercube Inc., Waterloo, Canada, 1996.

(17) In several previous publications including ref 12, the band gap was determined from the very onset of absorption (see, for example: McCullough, R. D.; Lowe, R. D.; Jayaraman, M.; Anderson, D. L. *J. Org. Chem.* **1993**, *58*, 904. Chen, T. A.; Rieke, R. *Synth. Met.* **1993**, *60*, 175.). However, since this procedure leads to rather large uncertainties, ΔE was determined from the maximum of the 0−0 transition and E_g by extrapolation to zero of the low-energy absorption edge, although these procedures lead to larger values than the previous one.

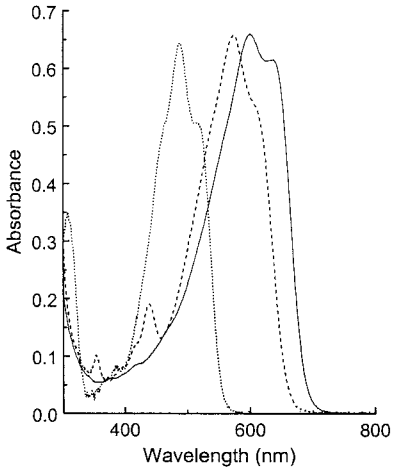

Figure 2. Electronic absorption spectra recorded in CH_2Cl_2: dotted line **4a**, dashed line **8a**, and solid line **16a**.

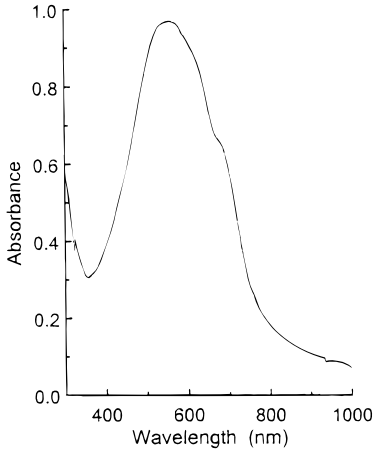

Figure 3. Electronic absorption spectrum for a film of **16a** on glass.

structure.[18] However, the vibronic structure is less resolved than for the analogue nTVs based on 3-octylthiophene or 3,4-dibutylthiophene,[12b] a difference that could be related to an enhancement of the vibrational disorder in the π-conjugated system caused by the dihexyl substituents. The large thermal ellipsoids observed for the hexyl carbons in the X-ray structure of Figure 1 appear consistent with this interpretation.

Unlike nTVs based on 3,4-dibutylthiophene,[12b] **4a**−**16a** exhibit excellent film-forming properties allowing the analysis of their solid-state electronic properties. Figure 3 shows as a representative example the UV−visible absorption spectrum of a thin film of **16a** cast on a glass slide from a CH_2Cl_2 solution. The spectrum exhibits a persistent vibronic fine structure consistent with a well-ordered material. The data in Table 1 show that the band gap (E_g)[17] of films of the longest oligomers (1.60 and 1.56 eV for **12a** and **16a**, respectively) are significantly smaller than that of the parent poly(thienylenevinylene) (PTV) prepared by the soluble precursor route (1.70−1.80 eV).[19] These results confirm in agreement with our previous conclusions,[12] that the ECL of PTV is limited to about eight TV units. On the other hand, the low band gap of oligomers **8a** to **16a** suggests that PTV prepared by thermal elimination contains a significant number of conjugation defects. This conclusion is supported by recent work on the parent poly(phenylenevinylene) prepared by the same route, which has demonstrated the strong dependence of the ECL and band gap on the conditions of thermal elimination.[20]

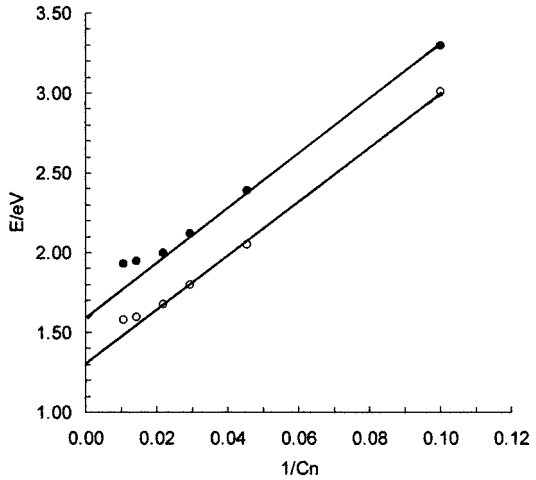

Figure 4. HOMO−LUMO gap (●) and band gap (○) for **2a**−**16a** vs the reciprocal number of carbons in the conjugated chain.

Figure 4 shows plots of ΔE and E_g vs 1/Cn for **4a**−**16a**. Extrapolation of the linear part to 1/Cn = 0 gives values of 1.60 and 1.30 eV for ΔE and E_g, respectively. However, for both series of data, a deviation from linearity occurs around Cn = 50−60 (10−12-mer) suggesting the existence of a convergence limit. Extrapolation of quantities such as ionization potential, electron affinity, oxidation potential, λ_{max}, ΔE, and E_g, determined on short-chain oligomers, has been widely used to analyze the chain length dependence of the electronic properties of π-conjugated oligomers and to predict the properties of an infinite defect-free polymer chain.[4,12] These extrapolations were based on the linear plot (1/Cn) of a hyperbolic function $f(n)$. However, as recently discussed by Meier et al., the existence of a finite ECL in linear π-conjugated systems implies the convergence of the above parameters toward a limiting value for a certain chain length.[21] Indeed, such a saturation limit has been observed for all series of oligomers investigated so far.[4c,f−h,5g,h] To evaluate the maximum ECL, Meier et al. have suggested that the ECL can be considered as reached when an incremental chain extension induces a red shift of λ_{max} or λ_{0-0} smaller than 1 nm.[21] On the basis of this definition, the 6-nm red shift of λ_{max} and the related decrease of ΔE between **12a** and **16a** shows that, although close, the saturation limit is not reached yet and that the ECL of dihexyl nTVs is at least equal to 94 sp^2 carbons (16-mer). Comparison of these results with the optical data for other classes of extended π-conjugated oligomers based on thiophene,[4f] 1,4-dialkoxyphenylenes,[4h] 1,4-phenyleneethynylenes,[1c] triacetylenes,[4g] and -2,5-thiopheneethynylenes[1c,5g,h] clearly shows that nTVs exhibit the longest ECL among known systems and the smallest ΔE value for both the 50-Å and the 100-Å range of chain length. These outstanding properties suggest that nTVs may be well suited as molecular wires in nanoscopic systems.

Cyclic Voltammetry. Table 2 lists the values of the apparent redox potentials ($E°_{app}1-E°_{app}6$) corresponding to the generation of the various cationic species for **4a**−**16a**. The CV of the dimer **2a** shows two irreversible anodic waves. As observed for other nTVs, the first oxidation step is in general followed

(18) Rughooputh, S. D. D. V.; Hotta, S.; Heeger, A. J.; Wudl, F. *J. Polym. Sci.* **1987**, *25*, 1071.

(19) (a) Yamada, S.; Tokito, S.; Tsuisui., T.; Saito, S. *Chem. Commun.* **1987**, 1448. (b) Barker, J. *Synth. Met.* **1989**, *32*, 43.

(20) Stenger-Smith, J. D.; Lenz, R. W.; Wegner, G. *Polymer* **1989**, *30*, 1048. Shah, H. V.; McGhie, A. R.; Arbuckle, G. A. *Thermochim. Acta* **1996**, *287*, 319. Herold, M.; Gmeiner, J.; Schwoerer, M. *Acta Polym.* **1996**, *47*, 436. Mertens, R.; Nagels, P.; Callaerts, R. *Synth. Met.* **1997**, *84*, 977.

(21) Meier, H.; Stalmach, U.; Kolshorn, H. *Acta Polym.* **1997**, *48*, 379.

Table 2. Cyclic Voltammetric Data for nTVs[a]

compd	$E°_{app}1$	$E°_{app}2$	$E°_{app}3$	$E°_{app}4$	$E°_{app}5$	$E°_{app}6$
2a	0.94	1.27				
4a	0.57	0.77				
6a	0.48	0.54	1.08			
8a	0.46		0.79	0.90		
12a	0.42		0.57		0.94	
16a	0.40		0.46		0.68	0.96

[a] Conditions: 10^{-4} M substrate in 10^{-1} M TBAHP in CH_2Cl_2; Pt electrodes, ref SCE; scan rate, 100 mV s^{-1}.

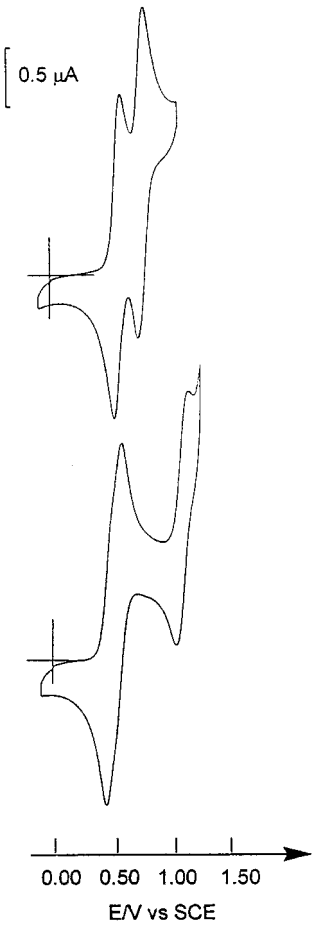

Figure 5. CVs of nTVs in 0.10 M TBAHP/CH_2Cl_2, $v = 100$ mV s^{-1}: top **4a** and bottom **6a**.

by the formation of a polymer.[22] However, due to the steric hindrance caused by interactions between hexyl chains during the cation radical coupling, rapid inhibition of electropolymerization occurs. With chain extension to the tetramer **4a**, the two oxidation processes become fully reversible (Figure 5), $E°_{app}1$ and $E°_{app}2$ shift negatively, and their potential difference decreases, indicating reduced Coulombic repulsion between positive charges in the dication. For **6a**, the two oxidation peaks almost merge into a single wave while a third reversible wave corresponding to the formation of the trication radical occurs ($E°_{app}3 = 1.07$ V). Coalescence of the two one-electron oxidation peaks into a two-electron wave occurs for **8a**, as confirmed by the 30-mV anodic/cathodic peak separation (Figure 6) and in agreement with previous results.[12] This two-electron process is followed by two one-electron waves corresponding to the successive generation of the trication radical and tetracation ($E°_{app}3$ and $E°_{app}4$ at 0.77 and 0.89 V, respectively). With further chain extension to **12a**, these two waves almost coalesce and a new one assigned to the pentacation radical occurs ($E°_{app}5 = 0.94$ V). For **16a**, the waves corresponding to the trication radical and tetracation fully coalesce into a second two-electron wave and the two successive two electron-waves draw nearer. Furthermore, $E°_{app}5$ shift negatively by 270 mV while a new reversible one-electron wave corresponding to the formation of the hexacation occurs around $E°_{app}6 = 0.96$ V.

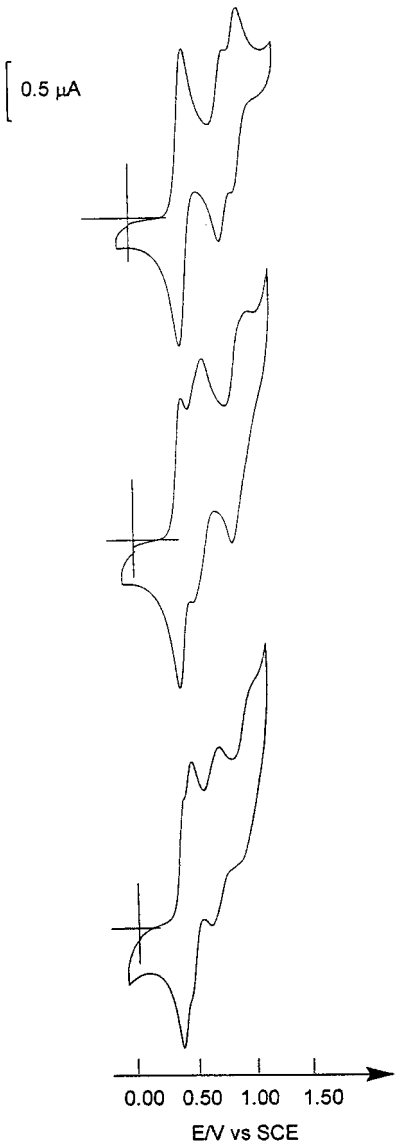

Figure 6. CVs of nTVs in 0.10 M TBAHP/CH_2Cl_2; $v = 100$ mV s^{-1}: top **8a**, middle **12a**, and bottom **16a**.

The chain length dependence of the electrochemical properties of nTVs is summarized in the diagram in Figure 7, which represents the variation of the $E°_{app}$ values of the various redox steps versus 1/Cn. The two convergence points at 1/Cn = 0.02 and 0.014 correspond to the coalescence of $E°_{app}1$ and $E°_{app}2$ (**8a**) and $E°_{app}3$ and $E°_{app}4$ (**12a**) into bielectronic transfers. Extrapolation of the linear part of $E_{pa}1$ vs 1/Cn to 1/Cn = 0 gives a value of 0.30 V/SCE for an infinite chain, in full agreement with previous results.[12b] However, a slight deviation from linearity occurs around 1/Cn = 0.015−0.020, (Cn = 50−60 carbons) and the location of the $E°_{app}1$ values for **12a** and **16a** above the straight line is consistent with the proximity of the saturation limit indicated by optical data. Extrapolation of the lines corresponding to the various oxidation steps suggests

(22) (a) Roncali, J.; Thobie-Gautier, C.; Elandaloussi, E.; Frère, P. *J. Chem. Soc., Chem. Commun.* **1994**, 2249. (b) Catellani, M.; Luzzati, S.; Musco, A.; Speroni, F. *Synth. Met.* **1994**, *62*, 223.

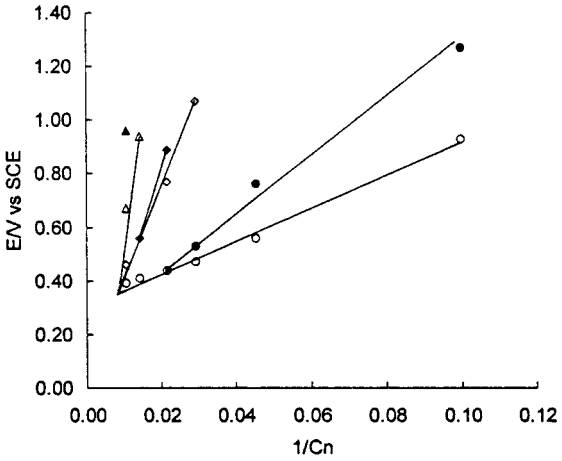

Figure 7. Variation of the $E°_{app}$ values for the various oxidation steps of nTVs vs the reciprocal number of carbons in the conjugated chain: (○) cation radical, (●) dication, (◇) trication radical, (◆) tetracation, (△) pentacation radical, and (▲) hexacation.

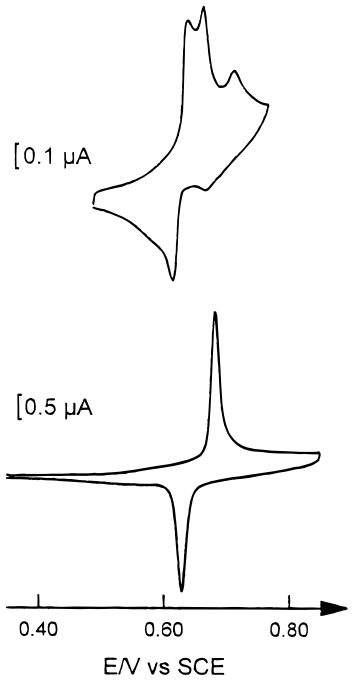

Figure 8. Solid-state CVs of films of **8a** (top) and **16a** (bottom) on Pt: electrolytic medium 0.10 M TBAHP/CH_3CN; $\nu = 50$ mV s^{-1}.

convergence toward a common potential limit around 1/Cn = 0.008 (120−130 carbons, 20−22-mer). This predicted chain length, which agrees well with the ECL indicated by optical data, should correspond to the single-step multielectronic oxidation of the whole π-conjugated system through a process similar to the p-doping of the parent polymer. Convergence of the $E°_{app}$ values corresponding to the cation radical and dication of oligothiophenes has already been observed for 1/Cn = 0.[4d] However, a major difference here is that convergence, which also includes the higher oxidation states, is predicted for a finite chain length (20−22 mer) which could eventually be synthesized.

To gain further information on the convergence process, the electrochemical behavior of nTVs has been analyzed in the solid state. Figure 8 shows the CV of films of **8a** and **16a** cast onto a platinum electrode from dichloromethane solutions. In both cases, the anodic peak undergoes a ∼0.30 V positive shift compared to the solution CV. Such a phenomenon has already been reported for oligophenylenes and oligothiophenes films by Heinze et al., who attributed this positive shift to the restriction imposed by the solid state to conformational changes from a twisted aromatic neutral state to a planar quinoid charged one.[23] This interpretation, which implies a more distorted structure in the solid state than in solution, appears in contradiction with (i) the fully planar structure observed in the crystal (Figure 1) and (ii) the fact that band gaps of solution-cast films are smaller than the corresponding ΔE values; this implies that film processing does not induce distortion in the π-conjugated system (Table 1). Consequently, in the absence of further evidence, we attribute the positive shift of the oxidation potential of the films to the extra energy required by the transport of charges and charge-compensating anions through an insulating compact material.

Further comparison of solution and solid-state CV for **8a** shows that while the first anodic peak shifts from 0.46 to 0.66 V, the second and third peaks shift negatively from 0.80 and 0.92 V in solution to 0.69 and 0.74 V, respectively in the film. In other words, the width of the potential window including the successive oxidation steps decreases from 460 mV in solution to 80 mV in the solid state. The same trend is observed for **12a** while for **16a** the four discrete oxidation steps observed in solution merge into a single redox system whose six-electron stoichiometry has been confirmed by coulometric measurements (see Experimental Section). Although the interpretation of this phenomenon is not straightforward, two extreme cases corresponding to inter- and intramolecular processes can be considered.

In the past few years, Miller et al. have extensively investigated the reversible dimerization of cation radicals of various series of oligothiophenes and discussed their possible role as alternatives for bipolarons in the interchain charge transport in PT.[24] Formation of π-dimers seems to be a rather general characteristic feature of π-conjugated oligomers, and several groups have reported spectroscopic or electrochemical evidences for cation radical dimerization.[25] Since the tendency to dimerize increases with chain length,[4f,25] a first possibility would be that oxidized long nTVs are also dimerized. In fact, it has been shown that the radical cation of long oligothiophenes such as the dodecamer are fully dimerized at temperatures lower than 50−60 °C.[4f] In the frame of this hypothesis, strong interchain attractive interactions could explain the coalescence of the various oxidation steps observed in the solid state for **16a** and the narrowness of the oxidation peak. However, the occurrence of one (**8a**) and two (**12a**, **16a**) bielectronic transfers implies that the first charged species capable of dimerizing is the trication radical for **8a** and the pentacation radical for **12a** and **16a**, and the strong interchain Coulombic repulsion that could result from the presence of three to five positive charges on each may represent an important obstacle to π-dimerization in solution.

An alternate explanation would be that the observed coalescence involves essentially an intramolecular recombination

(23) (a) Meerholz, K.; Heinze, J. *Angew. Chem., Int. Ed. Engl.* **1990**, *29*, 692. (b) Meerholz, K.; Gregorius, H.; Müllen, K.; Heinze, J. *Adv. Mater.* **1994**, *6*, 671. (c) Meerholz, K.; Heinze, J. *Electrochim. Acta* **1996**, *41*, 1839.

(24) (a) Hill, M. G.; Mann, K. R.; Miller, L. L.; Penneau, J. F. *J. Am. Chem. Soc.* **1992**, *114*, 2728. (b) Hill, M. G.; Mann, K. R.; Miller, L. L.; Penneau, J. F.; Zinger, B. *Chem. Mater.* **1992**, *4*, 1106. (c) Zinger, B.; Mann, K. R.; Hill, M. G.; Miller, L. L. *Chem. Mater.* **1992**, *4*, 1113. (d) Yu, Y.; Gunic, E.; Zinger, B.; Miller, L. L. *J. Am. Chem. Soc.* **1996**, *118*, 1013. (e) Graf, D. D.; Duan, R. G. Campbell, J. P.; Miller, L. L.; Mann, K. R. *J. Am. Chem. Soc.* **1997**, *119*, 5888.

(25) (a) Bäuerle, P.; Segelbacher, U.; Maier, A.; Mehring, M. *J. Am. Chem. Soc.* **1993**, *115*, 10217. (b) Hapiot, P.; Audebert, P.; Monnier, K.; Pernaut, J.-M.; Garcia, P. *Chem. Mater.* **1994**, *6*, 1549.

mechanism. This second hypothesis is supported by the narrow potential window in which the successive oxidation steps of **16a** occur in solution (0.60 V) and by the trend expressed by the diagram in Figure 7 which suggests that a rather limited increase in ECL is required to reach the full coalescence of all redox states. In the frame of this hypothesis, the passage from the solution to the solid state would contribute to increase the planarity and rigidity of the conjugated chain, thus leading to the enhancement of ECL needed for an intrachain recombination of the various redox states.

It should be underlined that these two situations represent extreme cases and that the real process may well involve a combination of intra- and intermolecular mechanisms. Furthermore, an absence of π-dimerization in solution does not necessarily exclude formation of π-dimers in the solid state, and finally, since it is evident that macroscopic charge transport in the film requires an interchain process, further work is clearly needed to clarify the original and complex behavior of this new class of extended oligomers.

Conclusion

The longest ever reported monodisperse π-conjugated nTVs have been synthesized. The ECL increases with chain length, and solution-processed films of the longest oligomers exhibit band gaps noticeably smaller than that of PTV and of the previously reported nTVs. Plots of the HOMO−LUMO and band gap vs inverse chain length reveal a deviation from linearity beyond the 10−12-mer suggesting a limit of convergence around the 20−22-mer.

Chain extension increases the number of accessible redox states and leads to a decrease of their potential difference with progressive coalescence of one-electron waves into bielectronic transfers. Thus, the 16-mer can be reversibly charged up to the hexacationic state via two two-electron and two one-electron steps within a 0.60-V potential window. Extrapolation of the potential of the various oxidation states vs inverse chain length suggests a possible common convergence limit corresponding to a single-step multielectronic oxidation step for the 20−22-mer. Such a single-step oxidation process is observed for solution-processed films of **16a**. Although further work is needed to elucidate the mechanisms responsible for this coalescence phenomenon, electrochemical and optical data suggest that intramolecular recombination plays an important role.

Comparison with data for other linear π-conjugated oligomers shows unequivocally that the ECLs of nTVs surpass that of any other known system of comparable dimensions, making nTVs well-suited candidates as molecular wires in nanoscopic systems. Whereas the absence of full saturation of ECL and the convergence predicted by extrapolation of optical and electrochemical data provide a strong incitement to synthesize longer nTVs, the proximity of the saturation poses the problem of the possible synthetic strategies allowing us to push back the limit of convergence and to reach systems with even larger ECLs. In this context, the significant decrease in bond length alternation and HOMO−LUMO gap recently demonstrated in bridged dithienylethylenes[26] suggests that application of this rigidification approach to extended nTVs could lead to π-conjugated oligomers with even smaller gaps. Work in this direction is now underway and will be reported in future publications.

(26) (a) Brisset, H.; Blanchard, P.; Illien, B.; Riou, A.; Roncali, J. *Chem. Commun.* **1997**, 569. (b) Blanchard, P.; Brisset, H.; Illien, B.; Riou, A.; Roncali, J. *J. Org. Chem.* **1997**, *62*, 2401.

Experimental Section

UV−visible absorption spectra were recorded on a Lambda 2 Perkin-Elmer spectrophotometer. Electrochemical experiments were carried out with a PAR 273 potentiostat−galvanostat in a three-electrode single-compartment cell equipped with platinum microelectrodes of 7.85×10^{-3} cm^2 area, a platinum wire counter electrode, and a saturated calomel reference electrode (SCE). Cyclic voltammetry was performed in methylene chloride solutions (HPLC grade) containing 0.10 M of tetrabutylammonium hexafluorophosphate (TBAHP) (Fluka puriss). Solutions were deaerated by argon bubbling prior to each experiment, which was run under inert atmosphere. The $E°_{app}$ values were determined after deconvolution of the CV (Condecon). For solid-state electrochemical experiments, films were cast on platinum electrodes of 0.25 cm^2 area from methylene chloride solutions and CV was performed in acetonitrile (HPLC grade) containing 0.20 M of TBAHP. Coulometric measurements for **16a** were performed on films cast using 2 μL of a 1×10^{-4} M methylene chloride solution. The average of 10 experiments gave a cathodic charge of $(1.5 \pm 0.3) \times 10^{-4}$ C (a redox process involving six electrons per molecule requires 1.2×10^{-4} C).

X-ray Structural Analyses. Crystal data for 4b: $C_{72}H_{112}O_2S_4$ (MW 1137.95) triclinic, *P*-1, $Z = 1$, $a = 9{,}094(3)$ Å, $b = 14.007(5)$ Å, $c = 14.302(6)$ Å, $\alpha = 84.25(3)°$, $\beta = 80.23(3)°$, $\gamma = 87.49(3)°$, $V = 1785(1)$ Å^3, $\rho_{calc} = 1.06$ g cm^{-3}.

Experimental Data and Structure Refinement. A dark red single crystal ($0.8 \times 0.5 \times 0.4$ mm^3) of **4b** was selected by optical examination, and X-ray diffraction data were collected at 298 K on an Enraf Nonius MACH3 four circles diffractometer. A total of 6539 reflections were measured in the $2° < \theta < 25°$ range by the zigzag ω scan technique (h −10.10; k −16.16; l 0.16; $\lambda = 0.710\,69$ Å). From 6263 independent reflections, 3538 with $I > 3\sigma(I)$ were deduced and used for structure refinement. After Lorentz and polarization corrections, the structure was solved with direct methods (SIR) which reveal all the non-hydrogen atoms. Finally, refinement of the structure (353 variables) leads to $R = 0.064$, $R_w = 0.092$ with the use of F magnitude; U_{ij} for S, C, and O atoms; x, y, z, and B fixed for H atoms.

General Synthetic Procedures. (a) Vilsmeier Formylation. In a round-bottomed flask kept under a nitrogen atmosphere are introduced the substrate compound dissolved in dry DCE and DMF. $POCl_3$ is added dropwise, and the mixture is then refluxed for at least 2 h. After cooling to room temperature, 1 M sodium acetate is added to neutrality and the mixture is stirred vigorously for 1 h. The solution is extracted with dichloromethane; the organic phase is dried over Na_2SO_4. After evaporation of the solvent, the crude product is purified by column chromatography.

(b) McMurry Coupling. In a round-bottomed flask, dry THF is introduced under a nitrogen atmosphere. After cooling to 0 °C, $TiCl_4$ is slowly added and the solution is stirred for 15 min at this temperature. Zinc powder is added portionwise, and the mixture is refluxed for 1 h. After cooling to 0 °C, a solution of the carbaldehyde and pyridine in dry THF is added and the mixture is refluxed for at least 2 h.

(c) Double Wittig−Horner Olefination. Under a nitrogen atmosphere, potassium *tert*-butoxide is added portionwise to a mixture containing the dicarbaldehyde and phosphonate **2e** in dry THF. The mixture is stirred at room temperature for 3 h. After solvent removal, the residue is taken up with CH_2Cl_2 and washed with water. After extraction of the aqueous phase with CH_2Cl_2, the organic phase is dried over Na_2SO_4 and filtered, and the solvent is evaporated under vacuum, and the crude product is purified by column chromatography and eventually recrystallized.

3,4-Dihexyl-2-thiophenecarboxaldehyde (1b). 3,4-Dihexylthiophene **(1a)** was prepared by Kumada coupling of bromohexylmagnesium and 3,4-dibromothiophene in the presence of $NidpppCl_2$, using a known procedure. The target compound **1b** was prepared by Vilsmeier formylation of **1a** (13 g, 51.5 mmol) using DMF (7.2 mL, 93 mmol) and $POCl_3$ (7.7 mL, 82.6 mmol) in 50 mL of dry 1,2-DCE. The usual workup and column chromatography (silica gel, CH_2Cl_2/essence G 1:1) gave 12.7 g (88%) of a yellow oil: ^{1}H NMR ($CDCl_3$, 500 MHz) δ 10.01 (s, 1H), 7.34 (s, 1H), 2.88 (t, 2H, $^3J = 7.8$ Hz), 2.54 (t, 2H, $^3J = 7.75$ Hz), 1.64−1.57 (m, 4H), 1.39−1.31 (m, 12H), 0.92−0.88 (m, 6H); ^{13}C NMR ($CDCl_3$, 270 MHz) δ 182.42, 151.34, 144.24, 138.03,

130.08, 31.65, 31.50, 31.39, 29.59, 29.13, 28.98, 28.09, 26.84, 22.44−22.40, 13.91−13.88; MS (EI) 280 ($M^{\bullet+}$, 100%); IR (KBr) 1662 (CHO) cm^{-1}. Anal. (calcd): C, (72.80) 73.08; H, (10.06) 10.08; S, (11.43) 11.18; O, (5.70) 5.70.

(*E*)-1,2-Bis[2-(3,4-dihexylthienyl)]ethylene (2a). **2a** was prepared by McMurry dimerization from **1a** (14 g, 50 mmol), $TiCl_4$ (8.25 mL, 75 mmol), Zn (9.81 g, 150 mmol), pyridine (7 mL), and 130 mL of dry THF; 12-h reflux and the usual workup and column chromatography (silica gel essence G) gave 12.5 g (94%) of a yellow oil which was then recrystallized in pentane at low temperature to give 9.8 g (74%) of a pale yellow solid: mp 50 °C; ^{1}H NMR ($CDCl_3$, 500 MHz) δ 7.00 (s, 2H), 6.75 (s, 2H), 2.60 (t, 4H, ^3J = 7.8 Hz), 2.49 (t, 4H, ^3J = 7.8 Hz), 1.63 (q, 4H, ^3J = 7.7 Hz), 1.50 (q, 4H, ^3J = 7.7 Hz), 1.40 (s, 8H), 1.35−1.33 (m, 16H), 0.93−0.90 (m, 12H); ^{13}C NMR ($CDCl_3$) δ 143.33, 139.80, 136.89, 119.66, 117.66, 31.76−31.64, 30.98, 29.69, 29.38−29.30, 29.07, 26.95, 22.66−22.65, 14.12; MS (EI) 528 ($M^{\bullet+}$, 100%). Anal. (calcd): C, (77.21) 77.42; H, (10.67) 10.92; S, (12.12) 12.14.

(*E*)-1-(5-Formyl-3,4-dihexyl-2-thienyl)-2-(3′,4′-dibutyl-2′-thienyl)-ethylene (2b). **2b** was prepared by Vilsmeier formylation from **2a** (4.75 g, 9 mmol) DMF (1 mL, 13 mmol), and $POCl_3$ (1 mL, 1.1 mmol) in 75 mL of dry 1,2-DCE. After the usual workup the residue was chromatographed (silica gel, CH_2Cl_2/essence G 4:6) to give 4.32 g (86%) of an orange oil: ^{1}H NMR ($CDCl_3$, 500 MHz) δ 9.97 (s, 1H), 7.28 (d, 1H, ^3J = 15.5 Hz), 6.96 (d, 1H, ^3J = 15.5 Hz), 6.84 (s, 1H), 2.85 (t, 2H, ^3J = 8 Hz), 2.62−2.56 (m, 4H), 2.49 (t, 2H, ^3J = 7.8 Hz), 1.67−1.33 (m, 32H), 0.93−0.85 (m, 12H); ^{13}C NMR ($CDCl_3$) δ 181.53, 152.73, 147.05, 143.54, 142.18, 141.25, 136.01, 134.64, 124.20, 119.74, 117.91, 32.28, 31.77, 31.68, 31.62, 31.57, 31.56, 31.23, 31.12, 29.68, 29.41, 29.38, 29.32, 29.29, 28.99, 27.13, 27.05, 26.37, 22.68, 22.63, 22.61, 14.12, 14.11, 14.10, 14.07; MS (EI) 556 ($M^{\bullet+}$, 100%); IR (KBr) 1653 (CHO) cm^{-1}.

(*E*)-1,2-Bis(5-formyl-3,4-dihexyl-2-thienyl)-2-(3′,4′-dibutyl-2′-thienyl)ethylene (2c). This compound was prepared by double Vilsmeier formylation of **2a** (3 g, 5.67 mmol), using DMF (2.8 mL, 36.2 mmol) and $POCl_3$ (2.4 mL, 25.7 mmol) in 75 mL of dry DCE. The usual workup and column chromatography (silica gel, dichloromethane/essence G 1:1) gave 2.9 g (89%) of an orange solid which was then recrystallized in pentane: mp 92 °C; ^{1}H NMR ($CDCl_3$, 500 MHz) δ 10.01 (s, 2H), 7.23 (s, 2h), 2.86 (t, 4H, ^3J = 7.8 Hz), 2.62 (t, 4H, ^3J = 7.6 Hz), 1.63−1.56 (, 4H), 1.34−1.32 (m, 16H), 0.93−0.89 (m, 12H); ^{13}C NMR ($CDCl_3$) δ 182.00, 152.75, 15.21, 143.41, 135.92, 122.46, 32.17, 31.47, 31.42, 31.27, 29.24, 27.02, 26.47, 22.50, 2.45, 22.34, 13.97; MS (EI) 584 ($M^{\bullet+}$, 100%); IR (KBr) 1646 (CHO) cm^{-1}; UV−visible (CH_2Cl_2) 420 nm. Anal. (calcd): C, (73.92) 73.68; H, (9.65) 9.60; S, (10.96) 10.74; O, (5.47) 5.37.

(*E*)-1-[5-(Hydroxymethyl)-3,4-dihexyl-2-thienyl]-2-(3′,4′-dibutyl-2′-thienyl)ethylene (2d). $NaBH_4$ (0.30 g, 8 mmol) was added portionwise at 0 °C to a solution of aldehyde **2b** (4 g, 7.2 mmol) in 50 mL of 1:1 CH_2Cl_2/methanol. The mixture was stirred for 15 min, diluted with CH_2Cl_2, and washed with water. After extraction with CH_2Cl_2, the organic phase was dried over Na_2SO_4, and the solvent evaporated. Column chromatography of the residue (silica gel, CH_2Cl_2/essence G 9:1) gave 3.65 g (91%) of a pale yellow solid which was then recrystallized in pentane: mp 60−61 °C; ^{1}H NMR ($CDCl_3$, 270 MHz) δ 6.97 (s, 2H) 6.75 (s, 1H), 4.74 (d, 2H, ^3J = 5.64 Hz), 2.61−2.45 (m, 8H), 1.64−1.32 (m, 32H), 0.93−0.89 (m, 12H); MS (FAB) 558 ($M^{\bullet+}$, 100%); UV−visible (CH_2Cl_2) λ_{max} 366 nm; IR (KBr) 3392 (OH), 1003 (C−O) cm^{-1}. Anal. (calcd): C, (75.21) 74.73; H, (10.46) 10.56; S, (11.47) 11.46; O, (2.86) 2.74.

(*E*)-1,2-Bis[2-(3,4-dihexyl-5-methylenediethylphosphonate)]-ethylene (2e). Diethyl phosphite (2.3 mL, 17.9 mmol) in 10 mL of dry THF was added dropwise to a suspension of NaH (0.72 g, 17.9 mmol) in 20 mL of dry THF under a nitrogen atmosphere at −20 °C, and the mixture was stirred for 1 h at this temperature. In the meantime, PBr_3 (0.14 mL, 1.5 mmol) was quickly added at −5 °C under nitrogen, to alcohol **2d** (2.5 g, 4.5 mmol) dissolved in 30 mL of 2:1 toluene/benzene. This second solution was added to the first one and the mixture refluxed for 2 h. After cooling to room temperature, the mixture was poured onto ice and extracted with Et_2O, and the organic phase was dried over Na_2SO_4. Removal of the solvent and column chromatography (silica gel, essence G/ethyl acetate 3:2) gave 2.43 g (73%) of a yellow solid: mp 50 °C; ^{1}H NMR ($CDCl_3$, 500 MHz) δ 6.94 (s, 2H), 6.73 (s, 1H), 4.12−4.06 (m, 4H), 3.29 (d, 2H, ^3J = 21.3 Hz), 2.59−2.54 (m, 4H), 2.48 (t, 4H, ^3J = 7.8 Hz), 1.61 (m, 2H, CH_2), 1.49−1.28 (m, 36H), 0.92−0.88 (m, 12H); MS (FAB) 678 ($M^{\bullet+}$, 100%); IR (KBr) 1060−1032 (P−O−R), 1239 (P═O) cm^{-1}. Anal. (calcd): C, (68.98) 69.76; H, (9.95) 9.91; S, (9.44) 9.40; O, (7.07) 7.04; P, (4.56) 4.58.

(*E,E,E*)-1,2-Bis[5-(3′,4′-dihexyl-2′-thienylvinyl)(3,4-dihexyl-2-thienyl)]ethylene (4a). This compound is prepared using the above-described procedure by McMurry dimerization of **2b** (3.2 g, 5.75 mmol) using $TiCl_4$ (0.7 mL, 6.3 mmol), Zn (0.83 g, 12.6 mmol), and pyridine (4 mL) in 60 mL of dry THF. The usual workup and column chromatography (silica gel, essence G/CH_2Cl_2 9:1) gave 2.68 g (86%) of a red solid which was recrystallized in 1:1 CH_2Cl_2/CH_3CN: mp 76 °C (dec); ^{1}H NMR ($CDCl_3$, 500 MHz) δ 6.99 (s, 4H), 6.98 (s, 2H), 6.76 (s, 2H), 2.64−2.56 (m, 12H), 2.49 (t, 4H, ^3J = 7.7 Hz), 1.63 (q, 4H, ^3J = 7.5 Hz), 1.56−1.51 (m, 12H), 1.41−1.35 (m, 48H), 0.93−0.90 (m, 24H); ^{13}C NMR ($CDCl_3$) δ 143.41, 141.48, 141.42, 139.99, 137.11, 134.99, 119.84, 119.37, 119.23, 117.90, 31.73, 31.58, 31.22, 31.18, 30.92, 29.63, 29.50, 29.36, 29.27, 29.02, 27.01, 26.88, 22.60, 14.14−14.07; MS (FAB) 1081 ($M^{\bullet+}$, 100%). Anal. (calcd): C, (77.71) 77.40; H, (10.43) 10.69; S, (11.85) 11.21.

(*E,E,E*)-1,2-Bis[5-(5′-formyl-3′,4′-dihexyl-2′-thienylvinyl)-2-(3,4-dihexylthienyl)]ethylene (4b). Prepared by Vilsmeier formylation of **4a** (3 g, 2.77 mmol), DMF (1.29 mL, 16.7 mmol), and $POCl_3$ (1.03 mL, 11 mmol) in 75 mL of dry 1,2-DCE. The usual workup and column chromatography (silica gel, CH_2Cl_2/essence G 7:3 + 2% Et_3N) gave 2.90 g (92%) of a red solid which was then recrystallized in 1:1 CH_2Cl_2/pentane: mp 143 °C (dec); ^{1}H NMR ($CDCl_3$, 270 MHz) δ 9.97 (s, 2H), 7.26 (d, 2H, ^3J = 15.5 Hz), 7.01 (s, 2H), 6.95 (d, 2H, ^3J = 15.5 Hz), 2.85 (t, 4H, ^3J = 7.8 Hz), 2.65−2.53 (m, 12H), 1.65−1.25 (m, 64H), 0.95−0.86 (m, 24H); ^{13}C NMR ($CDCl_3$) δ 181.64, 152.90, 147.12, 144.01, 142.65, 141.48, 136.79, 134.70, 134.36, 32.26, 31.62, 31.52, 31.49, 31.14, 31.04, 29.40, 29.33, 29.24, 29.20, 27.17, 22.61, 22.58, 22.54, 14.14, 14.11, 14.06, 14.02; MS (FAB) 1137 ($M^{\bullet+}$, 100%); IR (KBr) 1649 (CHO), 1589 (C═C trans) cm^{-1}.

(*E,E,E,E,E*)-1,2-Bis{5-[5′-(3″,4″-dihexyl-2″-thienylvinyl)(3′,4′-dihexyl-2′-thienylvinyl)]-3,4-dihexyl-2-thienyl}ethylene (6a). Prepared from **2c** (0.71 g, 1.21 mmol), **2e** (1.88 g (2.77 mmol), and *t*BuOK (0.72 g, 6.40 mmol) in 50 mL of dry THF. The usual workup and column chromatography (silica gel, CH_2Cl_2/essence G 7:3 + 2% Et_3N) gave 1.66 g (84%) of a dark red solid which was recrystallized in 1:1 $CHCl_3$/CH_3CN: mp 134 °C (dec); ^{1}H NMR ($CDCl_3$, 500 MHz) δ 7.00 (s 10H), 6.77 (s, 2H), 2.65−2.57 (m, 20H), 2.50 (t, 4H, ^3J = 7.7 Hz), 1.63 (q, 4H, ^3J = 7.7 Hz), 1.56−1.52 (m, 20H), 1.43−1.34 (m, 72H), 0.95−0.91 (m, 36H); MS (FAB) 1634 (M + 1). Anal. (calcd): C, 76.82 (77.88); H, 10.16 (10.36); S, 11.57 (11.77).

(*E,E,E,E,E*)-1,2-Bis-{5-[5′-(5″-formyl-3″,4″-dihexyl-2″-thienylvinyl)-(3′,4′-dihexyl-2′-thienylvinyl)]-3,4-dihexyl-2-thienyl}ethylene (6b). **6b** was prepared by Vilsmeier formylation of **6a** (1 g, 0.61 mmol), DMF (0.28 mL, 3.68 mmol), and $POCl_3$ (0.23 mL, 2.45 mmol) in 50 mL of dry 1,2-DCE. The usual workup and column chromatography (silica gel, CH_2Cl_2/essence G 7:3 + 2% Et_3N) gave 0.99 g of a solid which was then recrystallized in 1:1 $CHCl_3$/pentane: yield 70%; mp 171 °C (dec); ^{1}H NMR ($CDCl_3$, 500 MHz) δ 9.98 (s, 2H), 7.27 (d, 2H, ^3J = 15.4 Hz), 7.04 (d, 2H, ^3J = 15.4 Hz), 7.00 (s, 2H), 6.98 (d, 2H, ^3J = 15.4 Hz), 6.95 (d, 2H, ^3J = 15.4 Hz), 2.86 (t, 4H, ^3J = 7.9 Hz), 2.65−2.60 (m, 20H), 1.61−1.33 (m, 96H), 0.95−0.91 (m, 36H); MS (FAB) 1690 (M + 1); IR (KBr) 1654 (CHO) cm^{-1}.

(*E,E,E,E,E,E,E*)-1,2-Bis{5-[5′-[5″-(3‴,4‴-dihexyl-2‴-thienylvinyl)-3″,4″-dihexyl-2″-thienylvinyl)]-3′,4′-dihexyl-2′-thienylvinyl]-3,4-dihexyl-2-thienyl}ethylene (8a). **8a** was prepared by double Wittig−Horner olefination from **4b** (1.4 g, 1.23 mmol), **2e** (1.84 g, 2.71 mmol), and *t*BuOK (0.55 g, 4.90 mmol) in 50 mL of THF. The usual workup and column chromatography (silica gel, CH_2Cl_2/essence G 7:3 + 2% Et_3N) gave 2.28 g (64%) of a violet solid which was recrystallized in 1:1 $CHCl_3$/EtOH: mp 171 °C (dec); ^{1}H NMR ($CDCl_3$, 500 MHz) δ 6.99 (s 14H), 6.76 (s, 2H), 2.61 (s 28H) 2.50 (t, 4H, ^3J = 7.6 Hz), 1.65−1.37 (m, 128H), 0.94−0.92 (m, 48H); MS (FAB) 2186 (M + 1). Anal. (calcd): C, (77.96) 77.69; H, (10.32) 10.25; S (11.72) 11.77.

(*E,E,E,E,E,E,E*)-1,2-Bis-{5-[5′-[5″-(5‴-formyl-3‴,4‴-dihexyl-2‴-thienylvinyl)(3″,4″-dihexyl-2″-thienylvinyl]-3′,4′-dihexyl-2′-thienylvinyl]-3,4-dihexyl-2-ethienyl}ethylene (8b). **8b** was prepared by Vilsmeier formylation from **8a** (1.5 g, 0.69 mmol) DMF (0.5 mL), and $POCl_3$ (0.4 mL, 4.30 mmol) in 50 mL of dry 1,2-DCE. The usual workup and column chromatography (silica gel, CH_2Cl_2/essence G 7:3 + 2% Et_3N) gave 1.14 g (74%) of a solid which was then recrystallized in 1:1 $CHCl_3$/EtOH: mp 201 °C (dec); ^{1}H NMR ($CDCl_3$, 270 MHz) δ 9.98 (s, 2H), 7.26 (d, 2H, ^3J = 15.3 Hz), 7.04 (d, 2H, ^3J = 15.5 Hz), 6.99 (s, 6H), 6.97 (d, 2H, ^3J = 15.5 Hz), 6.95 (d, 2H, ^3J = 15.5 Hz), 2.88−2.82 (t, 4H, ^3J = 7.7 Hz), 2.61−2.51 (m, 28 H), 1.57−1.23 (m, 128 H), 0.96−0.85 (m, 48H); MS (FAB) 2242 (M + 1, 100%); IR (KBr) 1653 (CHO) cm^{-1}.

Oligomer 12a. **12a** was prepared by double Wittig−Horner olefination from dicarbaldehyde **8b** (0.80 g, 0.36 mmol), phosphonate **2e** (0.53 g, 0.78 mmol), and *t*BuOK (0.16 g, 1.43 mmol) in 30 mL of dry THF. After the usual workup and column chromatography (silica gel, CH_2Cl_2 + 2% Et_3N), the product was washed with ethanol in a Soxhlet and recrystallized in 1:1 $CHCl_3$/EtOH to give 0.64 g (55%) of a dark blue solid: mp 224 °C (dec); ^{1}H NMR ($CDCl_3$, 270 MHz) δ 7.03 (s, 22H), 6.79 (s, 2H), 2.64 (s, 44H), 2.52 (t, 4H, ^3J = 7.6 Hz), 1.66−1.29 (m, 192H) 1.00−0.92 (m, 72H); MS (MALDI-TOF) 3295.37. Anal. (calcd): C, (78.04) 77.79; H, (10.28) 10.30; S, (11.68) 11.64.

Dialdehyde 12b. **12b** was prepared by Vilsmeier formylation from **12a** (0.70 g, 0.21 mmol), DMF, (0.2 mL), and $POCl_3$ (0.14 mL, 1.50 mmol) in 50 mL of dry 1,2-DCE. After the usual workup and column chromatography (silica gel, CH_2Cl_2/essence G 7:3 + 2% Et_3N) the product was washed with pentane in a Soxhlet to give 0.29 g (40%) of a dark blue solid: ^{1}H NMR ($CDCl_3$, 270 MHz) δ 9.97 (s, 2H), 7.27 (d, 2H, ^3J = 15.5 Hz), 7.04 (d, 2H, ^3J = 15.5 Hz), 6.99 (s, 14H), 6.96 (d, 2H, ^3J = 15.5 Hz), 6.95 (d, 2H, ^3J = 15.5 Hz), 2.85 (t, 4H, ^3J = 7.5 Hz), 1.58−1.16 (m, 192H), 0.96−0.83 (m, 72H); IR (KBr) 1646 cm^{-1} (C═O).

Oligomer 16a. **16a** was prepared by double Wittig−Horner olefination from **12b** (0.35 g, 0.10 mmol), phosphonate **2e** (0.15 g, 0.23 mmol), and *t*BuOK (0.04 g, 0.31 mmol) in 30 mL of dry THF. After the usual workup the crude product was washed with ethanol and pentane in a Soxhlet and recrystallized in 1:1 $CHCl_3$/EtOH giving 0.14 g (30%) of a dark solid: mp 250 °C (dec); ^{1}H NMR ($CDCl_3$, 500 MHz) δ 7.00 (s, 30H), 6.77 (s, 2H), 2.62 (s, 60H), 2.50 (t, 4H, ^3J = 7.4 Hz), 1.64−1.38 (m, 256H), 0.95 (s, 96H); MS (MALDI-TOF) 4402.4. Anal. (calcd): C, (78.08) 77.58; H, (10.26) 10.19; S, (11.66) 11.42.

Supporting Information Available: ORTEP and tables of bond distances and angles, positional parameters, and general displacement parameters for **4b** (5 pages). Ordering information is given on any current masthead page.

JA980603Z